Journal of Materials Science: Materials in Electronics (2019) 30:20166–20173
https://doi.org/10.1007/s10854-019-02399-2

Synthesis, thermolysis, and solid spherical of RDX/PMMA energetic composite materials

Xinlei Jia[1] · Qing Cao[1] · Wenjie Guo[1] · Chao Li[1] · Jianjun Shen[1] · Xiaoheng Geng[1] · Jingyu Wang[2] · Conghua Hou[2]

Received: 2 May 2019 / Accepted: 16 October 2019 / Published online: 23 October 2019

Abstract
To improve the safety of cyclotrimethylenetrinitramine (RDX), a novel method for the improvement of nano-energetic materials was reported in our research. Based on the mature microcapsule technology, nano-energetic materials are firstly fabricated by using RDX as core material and poly methyl metharylate (PMMA) as shell material via an emulsion polymerization method. The RDX/PMMA nano-composites were characterized by scanning electron microscopy (SEM), Fourier-transform infrared (FT-IR) spectra, X-ray diffraction (XRD), differential scanning calorimetry (DSC) and impact sensitivity test, respectively. The SEM results indicated successful coating of the wall material PMMA on the surface of the core RDX, and the resultant particles by emulsion polymerization were regular solid spherical particles with smooth surface and dense coating layer, more importantly, it exhibits a very uniform particle size distribution with a narrower grain size. The XRD and FT-IR analyses did not show any change in the crystal structure after coating, thus indicating that PMMA could not change the crystal structure of RDX. Moreover, the characteristic height H_{50} of RDX/PMMA microspheres increased from 24.3 to 39.7 cm, significantly improving the safety performance. According to the DSC analysis, the T_b after core–shell coating increased by about 2 °C, and the Ea increased by 19.07 kJ mol^{-1}, revealing desirable thermal stability. It is obvious that the emulsion polymerization method is an effective desensitization technique to prepare core–shell composite particles for RDX.

1 Introduction

Microcapsule technology sprouted in the 1930s and developed rapidly in the mid-1970s. Nowadays, it has been listed internationally as a key high-tech in the twenty first century [1]. As a mature particle coating technique, it is widely used in pharmaceutical [2], food [3], paper [4], and textile industries [5] recently. However, few works have been done to explore its applications in the field of energetic materials at home and abroad. In principle, the microencapsulation method can be used for high-energy explosives as long as the coated core material is compatible with the coating method. Among them, emulsion polymerization is one of the commonly used methods for microcapsule technology, and the technique for producing polymer particles is generally based on emulsion polymerization in an aqueous system [6, 7]. It is usually limited to the preparation of certain polymers like poly methyl metharylate (PMMA), but not suitable for all polymers. Emulsion polymerization requires a variety of chemicals, such as monomers, initiators, emulsifiers and stabilizers [8], which is why we rarely see microcapsule technology applied to energetic materials. PMMA is an non-toxic and environmentally friendly material with the advantages of smooth surface, small specific gravity, high strength, corrosion resistance and good insulation performance [9]. And it exhibits a higher glass transition temperature and can be used to improve the mechanical strength of the system. Owing to its excellent thermal stability, chemical safety and aging resistance, PMMA is not only applicable to pharmaceutical encapsulation, but also gradually develop into medicine, food adhesives and other fields.

However, as a coating material, few studies have involved the application of PMMA in energetic materials. In our paper, taking MMA and RDX as the reactive monomer and the core material respectively, PMMA/RDX nano-energetic

✉ Xinlei Jia
1004024260@qq.com

✉ Jingyu Wang
wjywjy67@163.com

[1] College of Chemical Engineering and Safety, Binzhou University, Binzhou 256600, Shandong, China

[2] School of Environment and Safety Engineering, Shanxi Engineering Technology Research Center for Ultrafine Powder, North University of China, Taiyuan 030051, Shanxi, People's Republic of China

composite particles were fabricated via in situ polymerization under the action of initiator. And the results prove that microcapsule technology can be successfully applied in the field of energetic materials.

Nano-energetic composites can be prepared by various approaches, including sol–gel method [10], solvent/non-solvent method [11], spraying evaporation method [12], and spray drying method [13]. Over the past few years, several nano-energetic materials have been fabricated in different ways. In 2012, Chen et al. [14] prepared SiO_2/AP/RDX nano-energetic composites, and found that the cryogen SiO_2 can promote the decomposition of ammonium perchlorate and enhance the interaction between AP and RDX. The same year, Li et al. [15] prepared GAP/RDX composite energetic materials by sol–gel method. And results showed that the resultant GAP/RDX produced more energy during the explosion and their impact sensitivity was lower than that of the original RDX, however, the SEM analysis indicated that the coated particles were irregular. In 2012, Qiu et al. [16] evaluated the feasibility of single-step production for HMX nanocrystals and characterized the shape, size, surface morphology and internal structure of the as-prepared particles. In 2017, Chongwei et al. [17] obtained nano-CL-20/HMX cocrystal explosive by using spry drying technology, and the impact sensitivity was significantly decreased.

Herein, we demonstrate a general and facile method for improving nano-energetic materials via emulsion polymerization method. PMMA/RDX nano-energetic materials were successfully prepared by emulsion polymerization in O/W emulsion system, and the molecular structure of most materials is shown in Fig. 1. The application of microcapsule technology in the field of energetic materials can not only improve the stability while maintaining the explosive activity, but also provide strong technical support for the research of ultrafine high explosives. Meanwhile, the oxidant sensitivity of high explosives can be reduced, thereby improving the reliability. In addition, it provides high security and stability for weapon systems and has major political, military and economic implications.

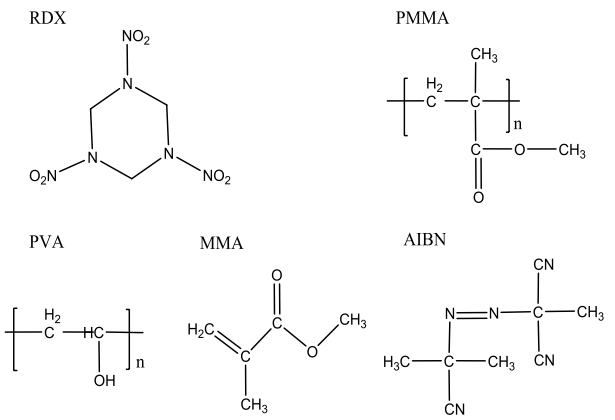

Fig. 1 Molecular structures of RDX, PMMA, PVA, MMA and AIBN

2 Experiment parts

2.1 Materials

RDX was provided by Gansu Yinguang Chemical Industry Group Co., Ltd. Methyl methacrylate (MMA) was obtained from Sinopharm Chemical Reagent Co., Ltd. Azobisisobutyronitrile (AIBN) and polyvinyl alcohol (PVA) were purchased from Tianjin guangfu Fine Chemical Industry Research Institute. Tween-80 and ethanol were from Tianjin Shen Tai Chemical Reagent Co., Ltd. Span-80 was obtained from Tianjin Damao chemical reagent factory.

2.2 Preparation of RDX/PMMA by water suspension coating technology

The preparation of RDX/PMMA by water suspension method is as follows: first, 3 g refined RDX was added into 120 ml distilled water to form RDX-water suspension solution under stirring. Second, a certain amount of PMMA was weighed and dissolved in ethyl acetate, formulating a solution with concentration.

Then, the as-prepared PMMA-ethyl acetate solution was uniformly added dropwise to the RDX-water suspension solution with M_{RDX}:M_{PMMA} of 97:3, and the mixture was stirred at a constant temperature for 2 h. At last, the solution was let to filter, followed by drying, finally affording high quality RDX/PMMA particles.

2.3 Synthesis of RDX/PMMA nano-energetic composites by microcapsule technology

The preparation of RDX/PMMA by microcapsule technology is as follows: first, prepare RDX emulsion. 3 g refined RDX was added to 120 ml distilled water, and then the self-made composite emulsifier was added dropwise. The mixture was emulsified with a high-speed emulsifier at a rate of 7000 rad/min for 3 min, forming a uniformly dispersed O/W emulsion system. Second, the initiator AIBN was added to the above emulsion. After stirring evenly, the MMA was added dropwise to the emulsion at a rate of 0.2 ml/min. During this process, the water temperature was slowly elevated to 75 °C with a water bath and the speed was adjusted to 350 rad/min. Then, the solution was let to react for 6 h in nitrogen atmosphere and then stand for 10 h in deionized water. After filtration and drying with a freeze dryer for 7 h, RDX/PMMA microcapsules were obtained. The schematic diagram are displayed in Fig. 2.

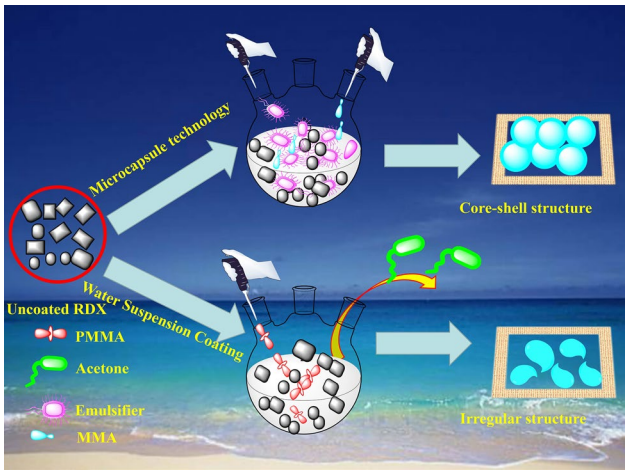

Fig. 2 The schematic diagram of the formation of RDX/PMMA by two methods

Figure 2 demonstrates the schematic of two methods for preparing RDX/PMMA. And the formation mechanism of the preparation of RDX/PMMA by microcapsule technology is as follows: Uncoated RDX is uniformly dispersed and MMA monomer is activated. with the addition of AIBN, the addition of AIBN "activates" the MMA monomer; under the catalysis, the MMA molecules are rapidly "identified" cross-linked with the uniformly dispersed RDX crystals, and then gradually deposited onto the surface of the RDX droplets to form a uniform coating. As the MMA prepolymer is continuously deposited and polymerized on the surface of the RDX, the coating layer is gradually densified and the coating is gradually completed, eventually forming RDX/PMMA composite particles.

In order to compare the RDX/PMMA fabricated by the two methods, we labeled the RDX/PMMA particles prepared by water suspension as RDX/PMMA-0.

3 Results and discussion

3.1 Characterization

Field-emission scanning electron microscopy (SEM) (Tescan MIRA3 LMH) was used to investigate the morphology, size and micro-structure of capsules. The as-prepared RDX/PMMA particles were dispersed on conductive carbon adhesive tapes to attach to a SEM stub, and then gold-coated. The crystal form of RDX/PMMA particles were detected by X-ray powder diffraction. X-ray powder diffraction (XRD) patterns were recorded on a Bruker D8 Advance diffractomerter with Cu Kα radiation. The infrared spectrum was measured on a Nicolet 380 Fourier transform infrared (FT-IR) spectrometer (KBr pellet, Thermo Fisher Scientific, Waltham, MA, USA). FT-IR transmission spectra were generated using an FTIR spectrophotometer (Nicolet 6700, Thermo Scientific). The thermal properties were characterized by a Setaran DSC-131 (Setaram, Hillsborough Township, NJ, USA). The conditions of DSC were as follows: sample mass: 0.7 mg; heating rate: 5, 10, 20 K/min; nitrogen atomosphere (flow rate: 20 ml/min). The impact sensitivity test conditions are: drop weight, 5 kg; sample mass, 35 mg. The impact sensitivity of each test sample was characterized by the drop height of 50% explosion probability (H_{50}). In this way, higher H_{50} value represents reduced impact sensitivity.

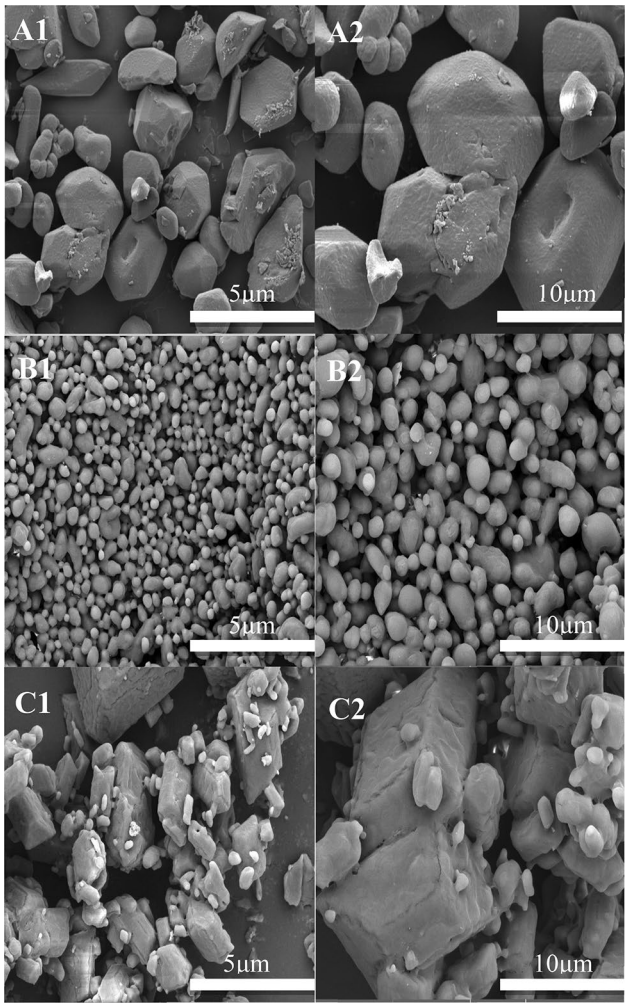

Fig. 3 SEM images of RDX particles: **a1**–**c1** low magnification SEM image and **a2**–**c2** high magnification SEM image

3.2 SEM morphological analysis of different RDX particles

The morphologies of the refined RDX (Fig. 3a), RDX/PMMA-0 (Fig. 3b) and RDX/PMMA (Fig. 3c) particles were compared and analyzed by scanning electron microscopy.

Figure 3 shows the SEM image of different RDX samples. It can be seen from A1 to A2 that the refined RDX particles have a smooth surface, but the crystal morphology is irregular and there is a phenomenon of particle concave; Interestingly, the nano-energetic composite particles prepared via emulsion polymerization are regular solid spherical particles with smooth surface and uniform dispersion (B1 and B2). And the coating is compact and there is no particle exposure. One reason for this phenomenon is that during the process of forming the emulsion, the vigorous mechanical agitation causes the refined RDX particles to collide with each other and form a uniform microcapsule core under the action of the emulsifier. And in the process of fabricating microcapsules via emulsion polymerization, MMA is able to form a uniform and dense wall on the surface of the uniformly dispersed emulsion system under the action of the initiator. More importantly, this is probably because the addition of the dispersant PVA decreases the surface tension of the water, and improves the wettability, thus increasing the affinity between RDX and PMMA. The Hamaker constant is minished simultaneously, and the attractive energy between particles is reduced, forming an effective steric hindrance. Besides, the repulsive energy between the composite particles rises, which greatly enhances dispersibility between the RDX/PMMA. While C1 and C2 shows that the RDX/PMMA-0 particles prepared by water suspension method are large and mutually bonded to each other, revealing a poor coating effect. The water suspension coating is a simple physical mixing process, and it is difficult to ensure that the binder can be uniformly dispersed on the surface of the RDX particles during the dropwise addition, which has been confirmed in many literatures [18–20].

In order to observe the core–shell structure and particle size of RDX/PMMA more intuitively, we performed SEM tests (e.g., Fig. 4) and particle size distribution measurements (as shown in Fig. 5) on the cross-sections and particle surfaces of the resultant RDX/PMMA particles. As shown in Figs. 4 and 5, we can clearly see that the surface distribution

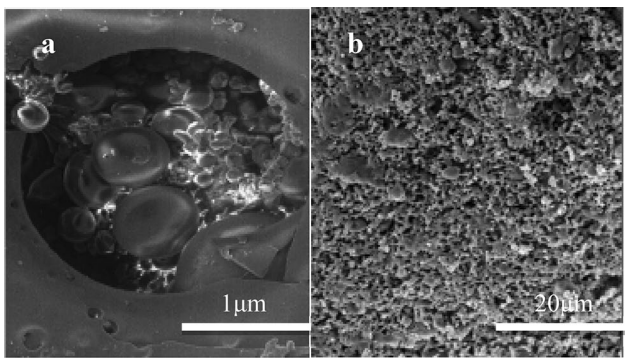

Fig. 4 SEM images of samples. **a** The cross section of RDX/PMMA. **b** The surface of RDX/PMMA

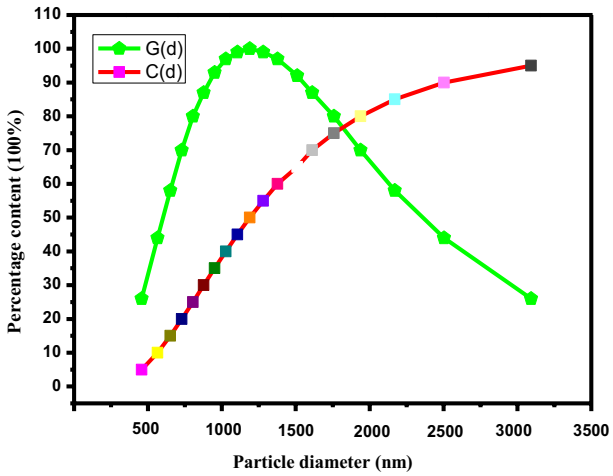

Fig. 5 Particle size distribution curves of RDX/PMMA

of RDX/PMMA particles is very dense, and that the inside of the particle is made up of a mixture of particles with a size range of 350–2.5 nm. This can be attributed to the fact that the content of MMA is only 3% during the fabrication of the composite particles, and we believe that RDX accounts for a large portion of these particles.

3.3 FT-IR and XRD analyses of different RDX particles

XRD and FT-IR analyses were adopted to investigate the crystal structure of the refined RDX, RDX/PMMA-0 and RDX/PMMA particles. And the results are as follows.

Figure 6 shows that the diffraction peaks of refined RDX (PDF Card 00-046-1606) and the as-prepared RDX/PMMA particles can correspond to those of the raw RDX, indicating that the crystal form of RDX does not change during the coating process. That is, the mechanical properties of the entire coating system are stabilized by changing the energy effect of the solid–liquid interface. The formation of PMMA binder under the physical action of van der Waals force between PMMA and RDX molecules will only aggravate the X-ray dispersion of XRD (the diffraction peak is broadened), but it will not damage the crystal structure of RDX. However, the intensity of the diffraction peak of the coated particles has weakened at the crystal plane 2θ of 13.1° (1, 1, 1), 17.87° (2, 0, 0), 29.33° (1, 3, 2), especially the diffraction peaks of the coated RDX/PMMA-0 and RDX/PMMA microcapsules become visibly broadened. This can be attributed to the "isotropic" physical properties [21] of the amorphous PMMA, resulting in an irregular arrangement for the resultant PBX particles in spatial distribution. Such periodic arrangement weakens the diffraction intensity of RDX. On the other hand, the stress effect makes the broadening of the peak obvious, and the addition of PMMA affects the

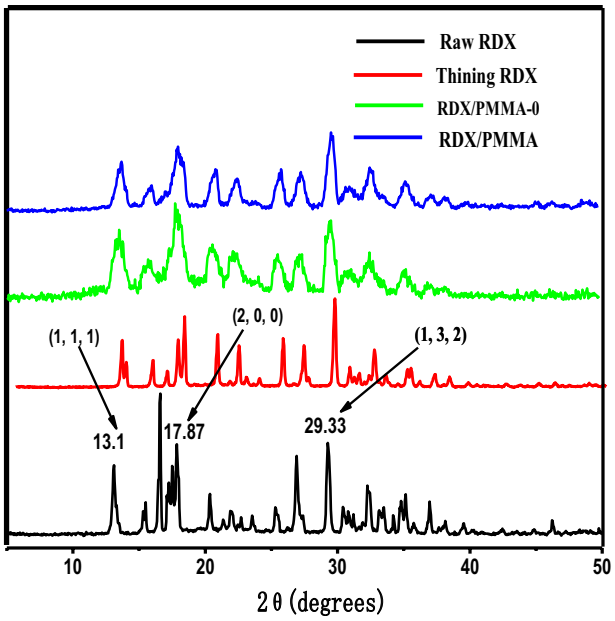

Fig. 6 XRD spectra of PMMA and RDX particles

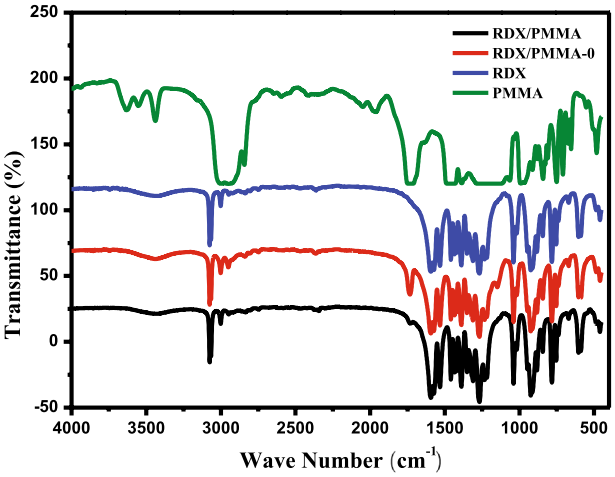

Fig. 7 FT-IR spectra of PMMA and RDX particles

lattice parameters of the RDX crystal (in some regions the lattice parameters are large, while in other regions the lattice parameters are small), resulting in the broadening of the diffraction peak of the composite particles in the figure [22].

FT-IR analyses were employed to identify the molecular structure of the samples. It can be seen from the infrared spectrum of RDX in Fig. 7 that there is $–CH_2$ stretching vibration absorption peak at 1400 cm^{-1}, 1450 cm^{-1}, 2950 cm^{-1} and 3100 cm^{-1}, and $–NO_2$ stretching vibration absorption appear near 1550 cm^{-1} and 1600 cm^{-1}. As can be seen, there is a distinct wide stretching vibration peak at 3500 cm^{-1} of FT-IR in Fig. 7. In fact, this peak does not exist in the infrared spectrum of PMMA. We think this peak should be a water peak (it is likely to come from KBr without drying). Moreover, it can be seen from the infrared spectrum of PMMA that there is C=O stretching vibration absorption peak at 1750 cm^{-1}, and –C=C– stretching vibration absorption appear at 2860 cm^{-1}. Interestingly, the characteristic absorption bands of RDX/PMMA-0 and RDX/PMMA contain the characteristic bands of RDX and PMMA, which means that PMMA is successfully coated on the RDX surface, corresponding to the XRD results.

3.4 DSC analysis of different RDX particles

DSC analysis was conducted to study the thermal properties of the refined RDX, RDX/PMMA-0 and RDX/PMMA. Their activation energies were calculated and the changes in thermal properties before and after refinement were analyzed. The results are displayed in Fig. 8. As shown in Fig. 8, for different heating rates, the refined RDX and the resultant nano-energetic materials have increased decomposition temperatures with the increase of heating rate. At the same heating rate, the peak temperature T_p of the refined RDX, RDX/PMMA-0 and RDX/PMMA particles changes slightly, indicating that PMMA has little effect on the decomposition temperature of RDX.

According to the DSC test data of RDX at the three heating rates, the decomposition kinetic parameters of RDX can be calculated by the Kissinger formula (1), Rogers formula (2) and Arrhenius formula (3) [23–26].

$$\ln\left(\frac{\beta_i}{T_{pi}^2}\right) = \ln\left(\frac{AR}{E_a}\right) - \frac{E_a}{RT_{pi}} \tag{1}$$

$$T_{pi} = T_{p0} + b\beta_i + c\beta_i \tag{2}$$

$$T_b = \frac{E - \sqrt{E^2 - 4RET_{p0}}}{2R} \tag{3}$$

where E_a is the apparent activation energy, A is the frequency factor, T is the absolute temperature, β is the heating rate, R is the gas constant, T_p is the peak temperature, and k is the decomposition rate constant at T.

It can be seen from Table 1 that compared with the raw RDX, both E_a and T_b of RDX/PMMA energetic composites prepared by water suspension coating and microcapsule technology are all increased, and the pre-exponential factors also have a corresponding increase. Specifically, the E_a of RDX/PMMA increased by 19.07 kJ mol^{-1} compared with that of the raw RDX, and increased by 9.94 kJ mol^{-1} compared with that of the RDX/PMMA-0. In the meantime, T_b of RDX/PMMA energetic particles is also increased. These indicate that the RDX/PMMA nano-energetic composites as

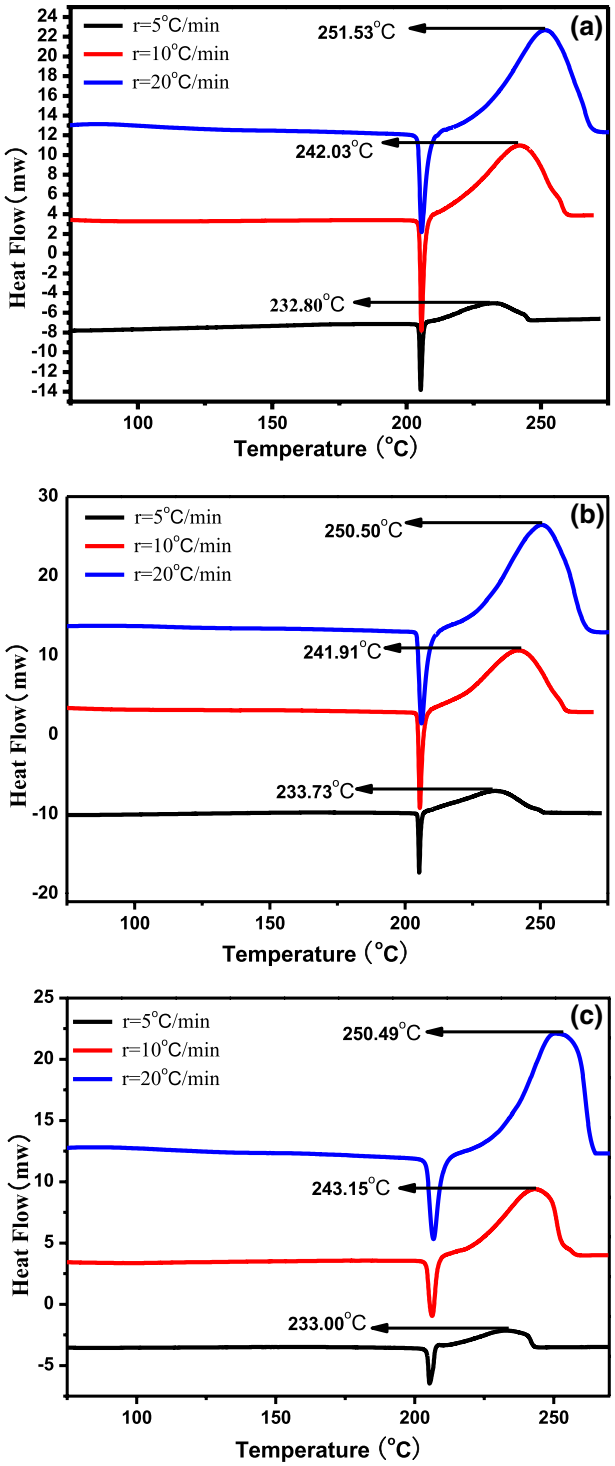

Fig. 8 DSC curves of RDX particles: **a** refined RDX; **b** RDX/PMMA-0; **c** RDX/PMMA

prepared by microcapsule technology exhibit better thermal stability. It can be explained in two aspects. On one hand, PMMA is uniformly distributed on the surface of RDX particles via emulsion polymerization, which affects the "local chemistry" effect during the thermal decomposition of RDX, thereby weakening the potential active site reaction center on the surface of RDX crystal. That is, the addition of PMMA causes the decomposition temperature of RDX to be delayed, which effectively decreases the thermal decomposition rate. On the other hand, the particle size of RDX/PMMA particles are significantly smaller than that of RDX/PMMA-0 particles. Therefore, for the same quality of RDX/PMMA particles, the former has a large specific surface area, resulting in a decrease in the adsorption capacity between the particles and an increase in the activation energy of the particles.

Table 1 Thermal decomposition kinetic parameters of different RDX samples

Samples	*Ea* (kJ mol^{-1})	log (A × S^{-1})	T_b (°C)	T_{p0} (°C)
Raw RDX	154.78	15.54	223.26	220.58
RDX/PMMA-0	163.91	16.49	223.48	220.95
RDX/PMMA	173.85	17.53	225.39	222.96

3.5 Analysis of the impact sensitivity

Impact sensitivity was also a key parameter to evaluate the safety performance of energetic materials. The impact sensitivities of the refined RDX, RDX/PMMA-0 and RDX/PMMA particles are separately tested according to GJB 722 A-1997 method 610. 302 tool. The impact sensitivity test results are listed in Table 2.

From Table 2, compared with raw RDX, the H_{50} of RDX/PMMA particles prepared by the two methods increased by 8.6 and 15.4 cm respectively, and the impact sensitivity decreased, thus improving the safety performance. This can be attributed to the hotspot theory [27–29]. On one hand, PMMA is successfully coated on the surface of RDX, which produced a certain buffering effect when impacted by a drop hammer, effectively slowing the formation of hot spots. On the other hand, the uniform small particle size distribution between the particles increases the gap between them. For the same quality of RDX, the increased force area will reduce the stress concentration between the particles, efficiently preventing the formation of the local hotspots. Since the particle size distribution of the RDX/PMMA particles

Table 2 Impact sensitivity of different RDX samples

Samples	Component (%)	H_{50} (cm^{-1})	Standard deviation (s)
Raw RDX	100	24.3	0.263
RDX/PMMA-0	97/3	32.9	0.381
RDX/PMMA	97/3	39.7	0.462

fabricated via microcapsule technology is more uniform, the effect of slowing down the formation of hot spots is more desirable. It can be concluded that a positive desensitization effect has been achieved after core–shell coating.

4 Conclusions

Herein, the mature microcapsule technology has been ingeniously applied to a new field-energetic materials. The RDX/PMMA nano-energetic composites were fabricated via emulsion polymerization, and their morphology and property were compared with those of RDX/PMMA particles prepared by water suspension coating. The following conclusions are drawn through comparative analysis. (1) In terms of morphology. The morphology of RDX/PMMA particles is much better than that of RDX/PMMA-0 particles. The former were solid spherical particles with smooth surface, dense coating and no particle exposure; while the latter exhibited a large coating defect, the particle morphology was irregular and mutually bonded with obvious angularity, showing poor coating effect. (2) In terms of performance. The RDX/PMMA particles are superior to RDX/PMMA-0 particles in both thermal and safety properties. The DSC results show that compared with the raw RDX, the E_a of RDX/PMMA nano-energetic particles prepared by the two methods increased from 154.78 to 163.91 kJ mol^{-1} and 173.85 kJ mol^{-1} respectively, and T_b increased from 223.26 to 223.48 °C and 225.39 °C respectively. The impact sensitivity test indicates that the characteristic height H_{50} of the RDX/PMMA particles fabricated by the two methods increased from 24.3 to 32.9 cm and 39.7 cm, respectively, and the latter showed more favorable safety performance. Therefore, a positive desensitization effect has been achieved after core–shell coating. It is foreseeable that microcapsule technology must have promising applications in the field of energetic materials in the future.

References

1. J. Qiao, Preparation and development of pharmaceutical microcapsules. Prog. Chem. **20**, 171–181 (2008)
2. M.T. Cook, G. Tzortzis, D. Charalampopoulos, V.V. Khutoryanskiy, Microencapsulation of probiotics for gastrointestinal delivery. J. Control. Release **162**, 56–67 (2012)
3. F. Nazzaro, P. Orlando, F. Fratianni, R. Coppola, Microencapsulation in food science and biotechnology. Curr. Opin. Biotechnol. **23**, 182–186 (2012)
4. F.R. Abdul Aziz, J. Jai, R. Raslan, Microencapsulation of essential oils application in textile: a review. Adv. Mater. Res. **1113**, 346–351 (2015)
5. Z.Q. Guo, H.E. Guo-Qiong, Y.D. Shi, Development and application of new dyeing technology of textile. Wool Text. J. **40**, 56–60 (2012)
6. N.P. Truong, J.F. Quinn, A. Anastasaki, Surfactant-free RAFT emulsion polymerization using a novel biocompatible thermoresponsive polymer. Polym. Chem. **8**, 1353–1363 (2017)
7. K.M. Meek, T.R. Eaton, N.A. Rorrer et al., Emulsion polymerization of acrylonitrile in aqueous methanol. Green Chem. **20**, 5299–5310 (2018)
8. K.J. Kim, Nano/micro spherical poly (methyl methacrylate) particle formation by cooling from polymer solution. Powder Technol. **154**, 156–163 (2005)
9. B. Charlot, S. Gauthier, A. Garraud, P. Combette, A. Giani, PVDF/PMMA blend pyroelectric thin films. J. Mater. Sci.: Mater. Electron. **22**, 1766–1771 (2011)
10. C. Teng, J. Wei, D. Ping, Facile preparation of 1,3,5,7-tetranitro-1,3,5,7-tetrazocane/glycidylazide polymer energetic nanocomposites with enhanced thermolysis activity and low impact sensitivity. RSC Adv. **7**, 5957–5965 (2017)
11. L. Xiao, S. Guo, H. Su, Preparation and characteristics of a novel PETN/TKX-50 co-crystal by a solvent/non-solvent method. RSC Adv. **9**, 9204–9210 (2019)
12. H. Qiu, V. Stepanov, S.A. Di, T. Chou, W.Y. Lee, RDX-based nano-composite microparticles for significantly reduced shock sensitivity. J. Hazard. Mater. **185**, 489–493 (2011)
13. L. Ning, B. Duan, X. Lu, Preparation of CL-20/DNDAP cocrystal by a rapid and continuous spray drying method: an alternative to cocrystal formation. CrystEngComm **20**, 2060–2067 (2018)
14. R. Chen, Y. Luo, J. Sun, G. Li, Preparation and properties of an AP/RDX/SiO2 nano-composite energetic material by the sol-gel method. Propellants Explos. Pyrotech. **37**, 422–426 (2012)
15. G. Li, M. Liu, R. Zhang, Synthesis and properties of RDX/GAP nano-composite energetic materials. Colloid Polym. Sci. **293**, 2269–2279 (2015)
16. H. Qiu, V. Stepanov, T. Chou, A. Surapaneni, A.R.D. Stasio, Single-step production and formulation of HMX nanocrystals. Powder Technol. **226**, 235–238 (2012)
17. A. Chongwei, L. Hequn, Y. Baoyun, Nano-CL-20/HMX cocrystal explosive for significantly reduced mechanical sensitivity. J. Nanomater **2017**, 1–7 (2017)
18. B.Y. Ye, C.W. An, J.Y. Wang, Formation and properties of HMX-based microspheres via spray drying. RSC Adv. **7**, 35411–35416 (2017)
19. C. An, F. Li, J. Wang, X. Guo, Surface coating of nitroamine explosives and its effects on the performance of composite modified double-base propellants. J. Propuls. Power **28**, 444–448 (2015)
20. Y.C. Lei, J.Y. Wang, Study on slurry coating technique for preparation of TATB/HMX based PBX. Chin. J. Explos. Propellants **38**, 59–62 (2015)
21. J. Zhang, L. Song, M. Sist, Chemical bonding origin of the unexpected isotropic physical properties in thermoelectric Mg_3Sb_2 and related materials. Nat. Commun. **9**, 4716–4725 (2018)
22. W. Ji, X. Li, J. Wang, B. Ye, C. Wang, Preparation and characterization of the solid spherical HMX/F_{2602} by the suspension spray-drying method. J. Energ. Mater. **34**, 357–367 (2016)
23. X. Liu, X. Liu, Y. Hu, Investigation of the thermal behaviour and decomposition kinetics of kaolinite. Clay Miner. **50**, 199–210 (2015)
24. X. Jia, J. Wang, Preparation and characterization of spherical submicron ε-CL-20 via green mechanical demulsification. J. Energ. Mater. **37**, 475–483 (2019)
25. Y. Zhang, C. Hou, X. Jia, Fabrication of nanoparticle-stacked 1, 1-diamino-2, 2-dinitroethylene (FOX-7) microspheres with increased thermal stability. J. Nanomater. **4**, 1–9 (2019)
26. R. Turcotte, M. Vachon, Q.S. Kwok, R. Wang, D.E. Jones, Thermal study of HNIW (CL-20). Thermochim. Acta **433**, 105–115 (2005)

27. B. Zygmunt, The detonation properties of explosive-water mixtures. Propellants. Explos. Pyrotech. **7**, 107–109 (2010)
28. B. Ye, C. An, Y. Zhang, One-step ball milling preparation of nanoscale CL-20/graphene oxide for significantly reduced particle size and sensitivity. Nanoscale Res. Lett. **13**, 42–49 (2018)
29. L. Borne, J. Mory, F. Schlesser, Reduced sensitivity RDX (RS-RDX) in pressed formulations: respective effects of intra-granular pores, extra-granular pores and pore sizes. Propellants. Explos. Pyrotech. **33**, 37–43 (2008)